Appl. Phys. B 52, 71–78 (1991)

Applied Physics B Photophysics and Laser Chemistry

Absolute Concentrations of Light Impurity Ions in Tokamak Discharges Measured with Lithium-Beam-Activated Charge-Exchange Spectroscopy

R. P. Schorn[1], E. Hintz[1], D. Rusbüldt[1], F. Aumayr[2], M. Schneider[2], E. Unterreiter[2], and H. Winter[2]

[1] Institut für Plasmaphysik der KFA Jülich GmbH, Association EURATOM/KFA, Postfach 1913, W-5170 Jülich, Fed. Rep. Germany
[2] Institut für Allgemeine Physik, TU Wien, Wiedner Hauptstrasse 8–10, A-1040 Wien, Austria

Received 10 June 1990/Accepted 19 October 1990

Abstract. We demonstrate the application of Li-CXS (fast lithium-beam-activated charge exchange spectroscopy) for measuring spatially and temporally resolved impurity ion concentrations in the TEXTOR tokamak edge plasma. After briefly describing the method of Li-CXS and its capabilities, we present a model for attenuation and atomic state population of an injected Li beam due to collisional interactions with the background plasma particles, taking into account up to eight excited LiI states for considering stepwise excitation-ionization processes.

Measured impurity radiation characteristics resulting from Li-activated CX of C^{q+} ($q = 5, 6$) in ohmically heated TEXTOR plasmas are evaluated with the above model and lead to the corresponding impurity ion concentrations within the TEXTOR edge region.

PACS: 52.70, 52.40M, 34.70

One of the crucial problems of nuclear fusion research is the influx of wall-released impurities into the hot plasma core of magnetic confinement devices. For a better control of this problem, the understanding of the ionization processes and of the transport of the impurity ions has to be improved and theoretical models have to be developed. At the present state of plasma theory, this requires in particular more knowledge about the spatial profiles of the different ionization stages of the impurities. Such information is difficult to obtain for plasma conditions as they exist in the transition region between the hot core and the wall of a magnetically confined plasma, i.e. the plasma boundary. It is characterized by steep gradients of the electron temperature, of the electron density and of the neutral densities. Local measurements of ion densities with a high spatial resolution are needed. A novel diagnostic method, the so-called "lithium-beam-activated charge exchange spectroscopy" (Li-CXS), which should be suited for this purpose, has been proposed by Winter in [1] and was applied for the first time at the TEXTOR tokamak at KFA Jülich.

Preliminary results, which were obtained for the C^{5+} ion, have been published in [2–4]. Meanwhile, the experimental setup, which suffered from several severe drawbacks, e.g. frequent arcing in the ion source and the lack of appropriate data acquisition and optical detection systems, has been improved considerably. Furthermore, the lithium beam's spatial population profiles of excited electronic levels and its attenuation by ionization when entering the plasma has satisfactorily been modelled for the particular TEXTOR conditions.

In the present paper, we describe practical experience with Li-CXS. In Sect. 1 we give a short review on the principles and capabilities of Li-CXS, which can supply time-resolved information on the background plasma density as well as the concentration and temperature profiles of impurity ions residing in the edge plasma. In Sect. 2 calculations of the electronic excitation and ionization of the injected Li atoms due to collisions with plasma particles are presented. These calculations are necessary for a quantitative evaluation of the observed signals. Section 3 describes the construction and operation of the Li-CXS diagnostic setup as used on TEXTOR. Finally, in Sects. 4 and 5 some typical measurements concerning density profiles of C^{5+} and C^{6+} are presented and evaluated, and the capability of Li-CXS for future edge plasma studies is discussed.

1. Principles and Capability of Li-CXS

If lithium atoms are injected into a tokamak edge plasma, diagnostic information can be obtained via two classes of excitation processes [5]. On the one hand, the injected Li atoms are excited by collisions with plasma particles, primarily electrons, and hydrogen ions (their respective

importance depending on the Li injection energy). The probability for excitation by electrons is proportional to the local electron density, but depends rather weakly on the electron temperature for typical tokamak plasma edge conditions ($T_e > 10$ eV). Therefore, at low Li injection energies ($E_{Li} < 5$ keV), where excitation by collisions with electrons is dominant, the perpendicular observation of LiI resonance emission along the injected beam gives direct access to the plasma electron density profile [6]. At higher beam energies also hydrogen ions contribute significantly to the population of the Li($2p$) level. Nevertheless, information about the electron density can still be deduced by using the model described in Sect. 2 in a self-consistent way. Moreover, spatially resolved measurements of the magnetic field strength can be made by virtue of the LiI resonance line Zeeman splitting [7], and the excitation of injected Li atoms with dye lasers tuned to forbidden transitions may supply information on local electric field strengths [8] as well.

On the other hand, impurity ions Z^{q+} residing in the edge plasma may capture the weakly bound outer electron from an injected Li atom into excited states, which subsequently decay rapidly under emission of characteristic impurity line radiation, from which the concentration of the particular impurity ion can be determined. Based on observations of this line emission and on calculations of the local Li(nl) state distribution along the injected beam, the spatially resolved density of any impurity ion can be evaluated.

Neutral beam-activated charge exchange spectroscopy has first been applied with hydrogen atoms utilizing either the neutral auxiliary heating beams or a dedicated diagnostic beam [9]. For probing the edge plasma, however, Li beams appear superior because of two reasons [1]. First, the relatively high density of neutral hydrogen in the edge region causes a strong background to the hydrogen-beam-produced impurity line radiation, whereas charge exchange with Li atoms ends up in systematically higher excited states of the impurity ions, which are also much less likely to be excited in background plasma-related collisional processes. Secondly, charge exchange with Li involves considerably larger cross sections than with neutral hydrogen atoms. Although these small cross sections can be compensated for by using high flux H^0 heating beams for diagnostic purposes, such heating beams are highly perturbing and can therefore be used for diagnostics only in a very limited sense. A Li beam, on the other hand, offers a truly non-perturbing tool at comparably moderate costs to investigate impurity concentrations at the plasma edge.

The signals from impact-excitation of injected Li atoms as well as from CX-induced excitation of impurity ions depend on the local flux of neutral Li atoms. For low beam energies ($E_{Li} < 2$ keV) a Li beam passing the edge plasma is attenuated primarily due to electron impact ionization. At higher beam energies interaction with plasma protons (electron capture from and proton impact ionization of Li) becomes the dominant attenuation mechanism [5]. As will be shown in Sect. 2, a detailed analysis of the attenuation has to take into account contributions from different excited Li states, but in the first approximation the attenuation can be estimated by considering ground state Li($2s$) only. For typical plasma temperatures T between 10 and 1000 eV the rate coefficients for the above mentioned processes (R_e^{ion}, R_p^{CX}, and R_p^{ion}) are almost independent of T [5], and therefore the probing depth d ($\equiv$ length for beam intensity attenuation to 1/e) accessible for a diagnostic Li beam into the edge plasma can be estimated from

$$d = \frac{v_{Li}}{\bar{n}_e \cdot (R_e^{ion} + R_p^{CX} + R_p^{ion})} \tag{1}$$

with v_{Li} being the velocity of the injected Li atoms and $\bar{n}_e$ the line-averaged plasma electron density (for a clean plasma $n_e \approx n_p$) along the Li beam path. Assuming for the tokamak edge plasma a typical density $\bar{n}_e \approx 10^{19}\ m^{-3}$ and using the rate coefficients of [5], we obtain

$d \leqq 0.1$ m for $E_{Li} \leqq 0.2$ keV,

$d \approx 0.2$ m for $1\ \text{keV} \leqq E_{Li} \leqq 40\ \text{keV}$.

With fast Li beams ($E_{Li} \geqq 100$ keV corresponding to $v_{Li} \geqq 1.7 \times 10^6\ ms^{-1}$) and moderate plasma densities, the probing depth is predicted to become as large as the plasma radius, whereas very slow Li beams (thermal effusion, $v_{Li} \approx 10^3\ ms^{-1}$; laser ablation, $v_{Li} \geqq 10^4\ ms^{-1}$ [2]) give access only to the outer part of the edge plasma. A probing beam of 20–30 keV kinetic energy as chosen in the present experiment is therefore suitable for investigations across the whole plasma edge on TEXTOR.

Electron capture from Li into multicharged ions mainly populates states with high angular momentum quantum numbers l [10]. However, for higher principal quantum numbers n, the different l states are almost degenerate and thus efficiently mixed by collisional processes inside the plasma [11]. Because of this mixing, an evaluation of absolute impurity ion concentrations using emission cross sections measured in single collision experiments [10] can be subject to considerable uncertainly.

2. Multi-State Model Calculations of the Injected Li beam Composition Across the Edge Plasma

For a further discussion it is useful to define a local plasma coordinate z along the injected Li beam such, that $z = 0$ at the entrance of the Li beam into the plasma.

In first approximation the local plasma electron density $n_e(z)$ (for a clean plasma $n_e \approx n_p$) can be correlated to the LiI 670.8 nm emission intensity $I_{671}(z)$ according to

$$I_{671}(z) = n_e(z) n_{Li(2s)}(z) \times (\langle \sigma^e_{671}(v^e_r) \cdot v^e_r \rangle + \langle \sigma^p_{671}(v^p_r) \cdot v^p_r \rangle). \tag{2a}$$

I_{671} is the number of photons emitted per unit of volume and time, the cross section σ_{671} covers all processes leading to LiI 670.8 nm emission [i.e. direct population of Li($2p$) by electron/proton impact and population of Li($2p$) via cascading from higher Li(nl) states, cf. Fig. 1], and v_r is the relative velocity between the plasma elec-

trons/protons (velocity v) and the injected monoenergetic Li atoms (velocity v_{Li}). The angular brackets indicate averaging over Maxwellian electron/proton velocity distributions $f(v)$, the result of which is a rate coefficient R:

$$\langle\sigma(v_r)\cdot v_r\rangle=\iiint d^3v\sigma(|\mathbf{v}-\mathbf{v}_{Li}|)\,|\mathbf{v}-\mathbf{v}_{Li}|f(\mathbf{v})\equiv R\,. \tag{2b}$$

As mentioned in the previous section, a quantitative evaluation of the background plasma density (from the LiI emission profile) and of impurity ion concentrations (from CX-produced characteristic line radiation) requires an accurate knowledge of Li(nl) state-resolved local densities $n_{Li(nl)}(z)$ along the injected Li beam, cf. Fig. 2. Knowledge of the radial $n_{Li(2p)}$ dependence then leads to an exact expression for the measured LiI 670.8 nm emission line intensity

$$I_{671}(z)=A_{2p\to 2s}n_{Li(2p)}(z) \tag{3}$$

with $A_{2p\to 2s}$ being the transition probability of spontaneous LiI 670.8 nm emission.

In order to determine the Li atomic state composition along the beam, the following boundary conditions are adopted.

$$n_{Li(2s)}(z=0)=n_{tot}\,, \tag{4a}$$

$$n_{Li(nl\neq 2s)}(z=0)=0 \tag{4b}$$

with n_{tot} being the initially injected Li(2s) atom number density. Due to the high energy of the beam its velocity can be taken as constant. As a consequence

$$n_{tot}=\sum_{nl}n_{Li(nl)}(z)+n_{Li^+}$$

$$(n_{Li^+}=\text{number density of Li ions}) \tag{4c}$$

is constant along the path of the beam.

Neglecting attenuation effects due to collisions with impurity ions in the plasma, the time evolution of the Li beam composition (i.e. of the densities of its various states), as seen by an observer moving with the injected Li atoms, can be described by a system of coupled linear differential equations (as used e.g. by Boley et al. [12] for the case of a H^0 diagnostic beam):

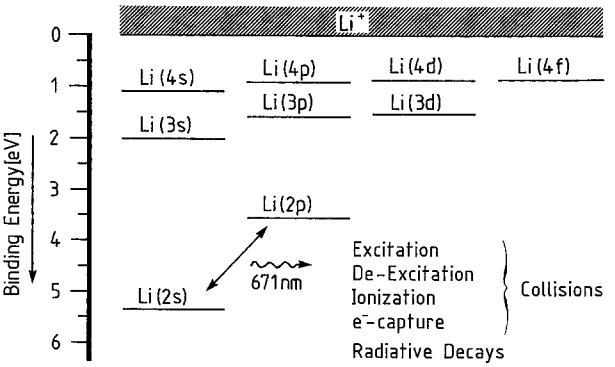

Fig. 1. Level diagram of the neutral lithium atom. All states shown [Li(2s) ground state, eight excited states and the ionized state] have been considered in the multi-state beam composition model

The following abbreviations and symbols are used in (5):

i	denotes specific neutral Li(nl) states;
$n_i(z)$	local number density of the state i;
$n_e(z), n_p(z)$	local number density of background plasma electrons and protons, respectively (for a clean plasma $n_e\approx n_p$);
R_e, R_p	rate coefficients for electron- and proton-related processes, Eq. (2b);
exc, dexc, ion	denotes excitation, de-excitation, and ionization, respectively;
$A(i\to j)$	transition probability for spontaneous emission $i\to j$.

It is important to note that, in general, the rate coefficients depend on the plasma temperature and thus on the position z.

By using the relation $\frac{dz}{dt}=v_{Li}$, Eq. (5) can be rewritten

$$\frac{dn_i}{dz}=\frac{1}{v_{Li}}F_i(z)\,. \tag{6}$$

The system of coupled linear differential equations (6) is then solved numerically, yielding the local densities $n_i(z)$ of

$$\frac{dn_i}{dt}=F_i(z)=-\underbrace{n_e\left[\sum_{j=i+1}^{m}R_e^{exc}(i\to j)+\sum_{j=1}^{i-1}R_e^{dexc}(i\to j)\right]n_i}_{\text{decrease of } n_i \text{ by electron-induced transitions}}-\underbrace{n_p\left[\sum_{j=i+1}^{m}R_p^{exc}(i\to j)+\sum_{j=1}^{i-1}R_p^{dexc}(i\to j)\right]n_i}_{\text{decrease of } n_i \text{ by proton-induced transitions}}$$

$$+\underbrace{n_e\left[\sum_{j=1}^{i-1}R_e^{exc}(j\to i)n_j+\sum_{j=i+1}^{m}R_e^{dexc}(j\to i)n_j\right]}_{\text{increase of } n_i \text{ by electron-induced transitions}}+\underbrace{n_p\left[\sum_{j=1}^{i-1}R_p^{exc}(j\to i)n_j+\sum_{j=i+1}^{m}R_p^{dexc}(j\to i)n_j\right]}_{\text{increase of } n_i \text{ by proton-induced transitions}}$$

$$-\underbrace{\sum_{j=1}^{i-1}n_iA(i\to j)}_{\text{decrease by spontaneous emission}}+\underbrace{\sum_{j=i+1}^{m}n_jA(j\to i)}_{\text{increase by spontaneous emission}}$$

$$-\underbrace{[n_eR_e^{ion}(i\to +)+n_pR_p^{ion}(i\to +)+n_pR_p^{CX}]n_i}_{\text{decrease by impact ionization and charge exchange}}\,. \tag{5}$$

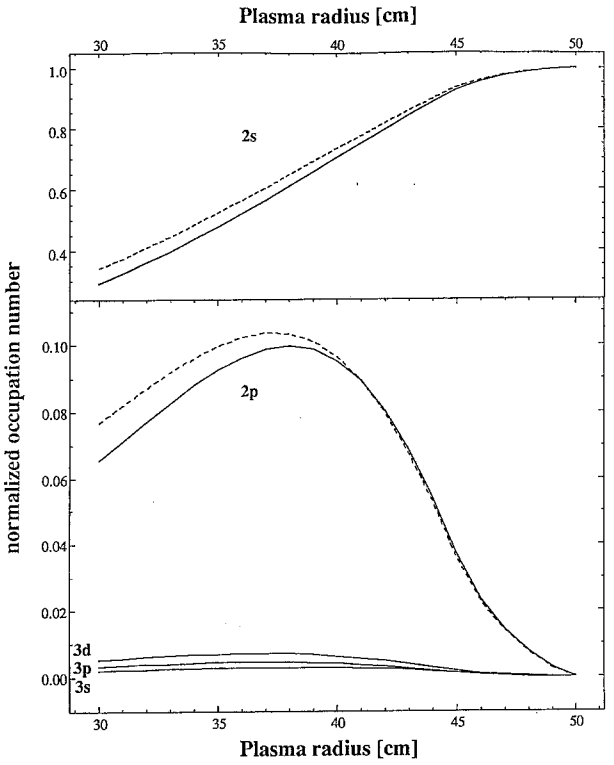

Fig. 2. Calculated lithium atomic state composition along the plasma radius. Since the contribution of the Li(4*l*) states is quite small, only the traces of the Li(2*l*, 3*l*) states are drawn. Broken lines indicate results obtained by using a 3-state model [Li(2*s*), Li(2*p*), Li^+, only]. Typical electron density and temperature profiles of ohmically heated TEXTOR plasmas have been assumed

all Li(*nl*) states. In Fig. 2, as an example, we show calculated normalized Li(*nl*) densities as function of the plasma radius, assuming n_e and T_e profiles of a typical ohmic tokamak edge plasma. These calculations can be checked by direct measurement of $n_{\mathrm{Li}(2p)}$, cf. (3).

In case of a non-negligible impurity ion content in the plasma it is also necessary to include relevant CX processes in the expression for $F_i(z)$:

$$F_i'(z) = F_i(z) - n_i(z) \sum_{\text{impurities}} \left(\sum_{q=1}^{q_{\max}} n_q(z) \langle \sigma_q^i v_r \rangle \right) \tag{5a}$$

with $n_q(z)$ being the local density of an impurity ion Z^{q+} and σ_q^i the total CX cross section for electron capture from Li(*nl*) into Z^{q+}.

In this case, quasi-neutrality of the plasma demands

$$n_e(z) = n_p(z) + \sum_{\text{impurities}} \left\{ \sum_{q=1}^{q_{\max}} q \cdot n_q(z) \right\}. \tag{7}$$

With the state composition of the Li beam being known along the whole penetration depth, any desired local impurity ion concentration can be evaluated from the corresponding characteristic line radiation intensity $S_\lambda(z)$, to which each atomic Li state contributes according to its density and relevant CX cross section

$$S_\lambda(z) = k_\lambda v_{\mathrm{Li}} n_q(z) \sum_i n_i \sigma_\lambda^i, \tag{8}$$

where σ_λ^i denotes the cross section for emission of characteristic photons with wavelength λ after state-selective CX population of a certain impurity ion state $Z^{(q-1)}(nl)$ by electron capture from an individual atomic Li state *i*. The parameter k_λ takes into account the wavelength-dependent efficiency of the spectroscopic detection system and has to be determined by an independent calibration.

Except for the Li(2*s*) ground state atoms there exist practically no measured cross sections or rate coefficients for excitation, ionization and electron capture, as needed in the coupled equations (5). Therefore, a critical evaluation of various empirical cross section formulae for such collisional processes involving impact of electrons and protons has been carried out [13]. Parameterized expressions have been derived to calculate all needed rate coefficients in the appropriate ranges of plasma temperatures and Li beam injection energies. The corresponding deexcitation rate coefficients have been obtained by assuming the principle of detailed balance and taking into account the statistical weights of involved states. For the lifetimes of excited atomic Li states tabulated values [14] have been utilized.

Finally, the total cross sections for electron capture σ_q^i from excited Li atoms into impurity ions Z^{q+} [used in (5a)] and the respective contributions σ_λ^i to emission at characteristic wavelength λ, cf. (8), have been estimated by scaling measured data for collisions of Z^{q+} with Li(2*s*) ground state atoms [10] according to results of empirical Landau-Zener (LZ) calculations [15], i.e.

$$\sigma^i = \sigma^{2s} \frac{\sigma^i(\mathrm{LZ})}{\sigma^{2s}(\mathrm{LZ})}. \tag{12}$$

Results of the above described model calculations [including up to nine Li(*nl*) states, cf. Fig. 2] for both the LiI 671 nm line emission and CX-produced line emission from selected impurity ions will be compared with measurements in Sect. 4.

3. Application of Li-CXS to the TEXTOR Tokamak

One important task of the research program of the tokamak TEXTOR at KFA Jülich is the characterization of the outer plasma regions. This includes the radial distributions of the different ionization states of the important impurity species. As pointed out in Sect. 1, Li-CXS is very well suited to investigate the latter items, as present day machines throughout involve low-*Z* materials in plasma-facing devices, such as carbon, boron, or beryllium.

A high current lithium beam injector has therefore been installed at TEXTOR. The device is capable of producing a neutral lithium beam of 20–30 keV energy and 5–10 mA total equivalent current at the plasma boundary, the beam diameter (FWHM) being about 40 mm at this location. In a HORDIS-type ion source [16], lithium vapour diffusing from an oven into the hot discharge chamber is ionized. The ions are extracted by a set of three grids, each one containing seven holes. The total beam diameter here is 19 mm. The beam is mass-

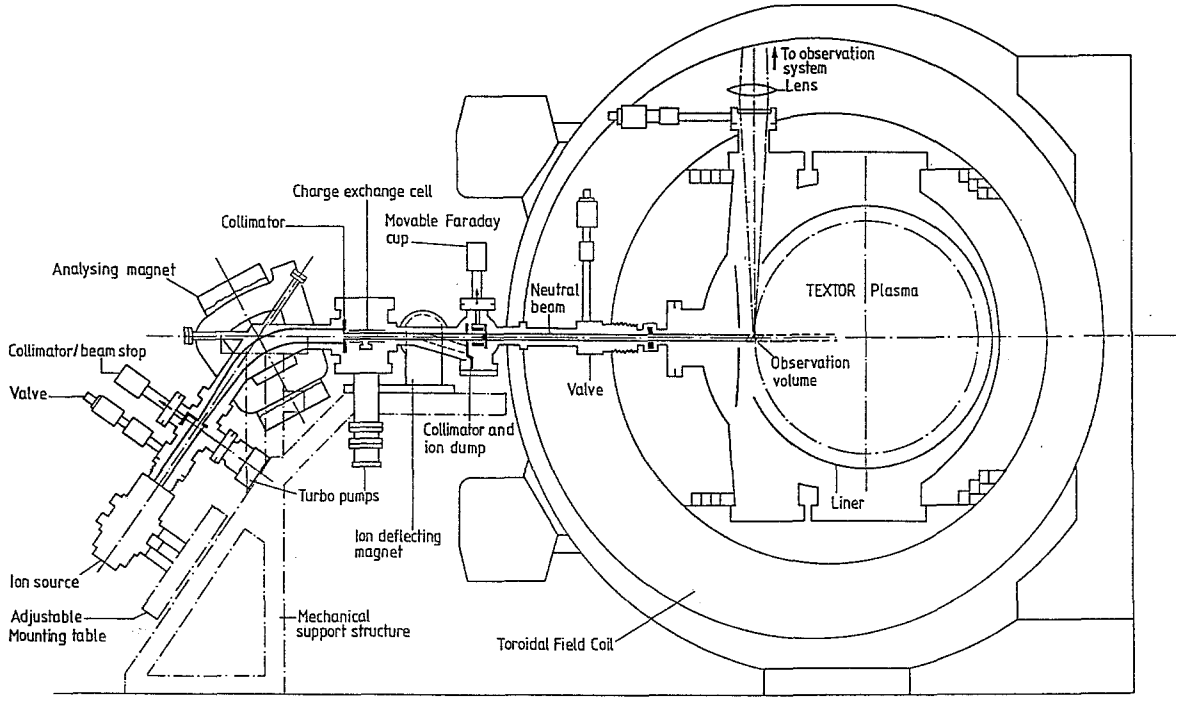

Fig. 3. Details of the 20 keV neutral lithium beam source as installed at the TEXTOR tokamak. A detailed description is available in [17]

analyzed in a focussing stigmatic analyzer magnet and then partially neutralized (~80% efficiency) by resonant charge exchange collisions in a thermal lithium vapour cell. The non-neutralized beam fraction is magnetically deflected onto an ion dump. The absolute lithium current is determined by means of a calorimetric Faraday cup close to the entrance to TEXTOR. Finally, the beam enters the plasma edge radially in the equatorial midplane of the torus.

To separate Li-CX excited radiation from the background radiation excited continuously by plasma particles, the arc voltage of the ion source discharge can be pulsed with frequencies up to 500 Hz. Consequently, the pulsed Li^0-beam produces a CX-modulation on a more or less constant collisional background radiation signal. Typical operation parameters, which were also used during the experiments described below, are 20 keV injection energy, 6 mA neutral current into TEXTOR, and a pulse frequency of 250 Hz (duty cycle 1:1). Under these conditions, the beam shows a probing depth of 25 cm into a typical ohmically heated TEXTOR plasma. Figures 3 and 4 show the experimental setup for beam generation and injection at TEXTOR. A more detailed description of the injector's properties and technical features is available in [17].

The Li-activated CX-radiation is detected spectrally, spatially and temporally resolved by means of a large aperture spectrometer at the end of a radiation transport system permitting a radial scan. Because all impurity species provide intense transitions in the visible, glass optics could be used throughout. A front-end doublet of 150 mm diameter images the Li^0-beam with unit magnification onto a field lens of 200 mm diameter. This picture of the beam is scanned by a galvo-driven mirror with 65 mm diameter, permitting scanning frequencies of up to 5 Hz. Almost the whole penetration region of the beam is accessible. An optical relay system further images the beam with a 2:1 reduction onto the slits of two monochromators, being separated by a dichroitic beam-splitter. Wavelengths below 600 nm are observed with a specially designed large grating spectrometer, which can be tuned to any desired CX line in the visible. The aperture ratio of the instrument is 1:5.5, the focal length is 800 mm, and the grating has 600 lines/mm, a size of 165×220 mm^2, and is blazed at 2700 nm. The spectrum can be shifted across the exit slit by means of a galvo-driven thick glass plate being tilted by an amount of up to $\pm 15°$, which permits an easy tuning to the line maximum and scanning of line profiles. The slit size was usually 1×20 mm^2. The LiI resonance

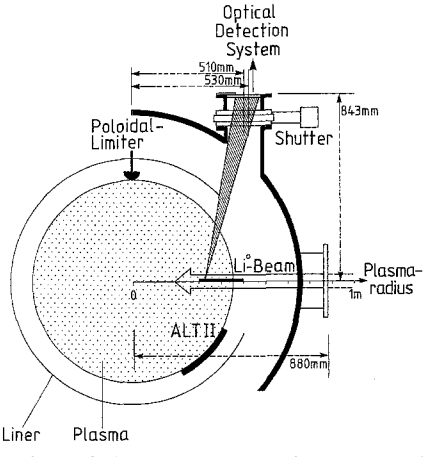

Fig. 4. Polar view of the TEXTOR section, where the Li-CXS experiment is situated. Details of the beam and observation geometry in the equatorial midplane are shown. "ALT II" is a toroidal belt limiter

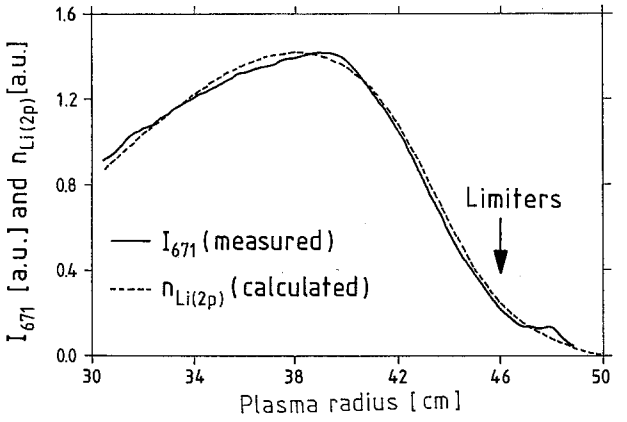

Fig. 5. Correlation of the measured LiI radial emission profile (resonance line at 670.8 nm) with the modelled density of the $2p$ state in the lithium beam (shot #38519). Both profiles are normalized to the same maximum

radiation ($2^2S \leftarrow 2^2P$) of the beam atoms is observed at 670.8 nm with a filter monochromator of 0.8 nm FWHM, having the same slit size as the spectrometer. Radial profiles of the LiI resonance radiation, induced by collisions of the beam atoms mainly with the plasma electrons, can be used either to calculate electron densities applying the technique described by Pospieszczyk et al. in [2, 18] or to check the reliability of the beam attenuation model outlined in Sect. 2. Because the emission intensity at 670.8 nm is proportional to the number of lithium atoms in the 2^2P-state (3), the recorded LiI profiles have to be compared with the modelled $n_{\mathrm{Li}(2p)}(z)$ profile. As a critical proof for the capabilities of the developed multi-state beam-attenuation model, Fig. 5 demonstrates excellent coincidence of a calculated $n_{\mathrm{Li}(2p)}(z)$ profile and an experimentally recorded LiI-emission profile of TEXTOR shot #38519. The n_e and T_e profiles needed to run the attenuation algorithm of Sect. 2 have been obtained by means of Thomson scattering (T_e, [19]), ablated atomic beam diagnostics (n_e and T_e, [2, 18]), and HCN laser interferometry (n_e, [20]). The obtained spatial resolution of 2 mm in TEXTOR is determined by the slits in front of the filter monochromator and the spectrometer.

The following raw signals are simultaneously digitized by an 8 channel data-logger with a sampling frequency of 10 kHz:

- PMT signal of the LiI line at 670.8 nm;
- PMT signal of the CX line (spectrometer);
- current measured at the ion dump (non-neutralized fraction of the beam);
- angle of the scanning mirror (z-position);
- angle of the tilted glass plate in the spectrometer (spectral position);
- primary TTL pulse used for the ion source discharge modulation (serves as a reference for signal demodulation);
- temperature of the calorimetric Faraday cup→neutral beam current).

The recorded raw data are stored and processed on a VAX 8800 computer. An appropriate software has been written to subtract the background signals with respect to the primary modulating TTL pulse as a reference. This kind of "digital lock-in" is able to extract the Li-CXS radiation even from an intense plasma background.

Finally, an absolute calibration of the optical detection system is necessary to evaluate local impurity densities $n_q(z)$ from (8). This is done by imaging a tungsten ribbon lamp onto the entrance slit of the spectrometer, using otherwise the same optical setup as during plasma shots. The boundary condition of (4a) implies the knowledge of the total Li^0 current at the very plasma edge. As mentioned before, this quantity is obtained from a calorimetric cup measurement.

4. Experimental Results: C^{q+} Profiles in Ohmically Heated TEXTOR Discharges

Li-CXS experiments have been carried out with a pulsed 20 keV neutral lithium beam of 6 mA equivalent current. In ohmically heated TEXTOR discharges, radial density profiles of C^{5+} and of fully stripped C^{6+} have been recorded. The discharges were performed at a plasma current of 340 kA, a line-integrated central electron density of 2.2×10^{13} cm^{-3} and a toroidal magnetic field of 2.25 Tesla. To ensure a maximum of toroidal profile symmetry, the plasma was operated solely with the toroidal belt limiter ALT II [21] positioned at a plasma radius of 46 cm. The profiles presented below have been obtained 8 weeks after boronization of TEXTOR. As the performance of the amorphous boronated carbon films (a-C/B : H) had significantly deteriorated after this period, especially on the graphite limiter surfaces, the plasma was predominantly contaminated with carbon, i.e. the boron content, which could influence CXS-signals of C^{5+} due to an overlapping of spectral lines, is expected to be rather low.

The following transitions and state-selective emission cross sections σ_λ^{2s} for charge exchange with the Li^0-groundstate have been employed:

imp. species	transition	wavelength	σ_λ^{2s} [10^{-15} cm^2]	Ref.
C^{5+}	$6h\,^{1,3}H^0 \leftarrow 7i\,^{1,3}I$	494.5 nm (C^{4+})	2.6	[10]
C^{6+}	$7i\,^2I \leftarrow 8k\,^2K^0$	529.0 nm (C^{5+})	3.5	(recent measurements [22])

For presentation, two shots have been selected from a longer series of experiments, which may serve as typical cases. At shot #39505, the spectrometer was tuned to the $C^{6+} \rightarrow C^{5+}$CX line of 529 nm. The other shot #39510 delivered $C^{5+} \rightarrow C^{4+}$CX signals at 494.5 nm. To demonstrate the ratio of Li-CX radiation to the plasma background, Fig. 6 shows a small time interval of recorded raw signals during shot #39510. The modulation caused by

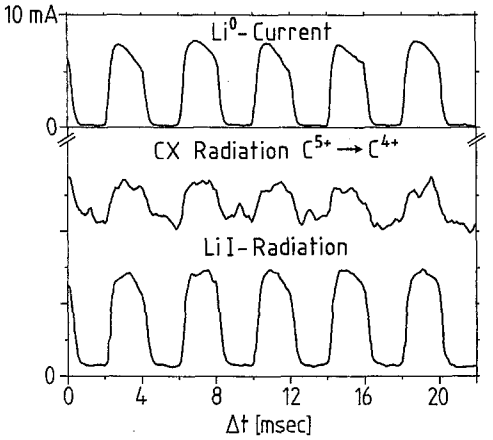

Fig. 6. Raw signals of shot #39510 in the flat-top phase 1s after the start of the discharge. At this time, the radial position of observation is 40 cm outward from the plasma center. A clear correlation of the CX-modulation to the Li^0 beam current is visible

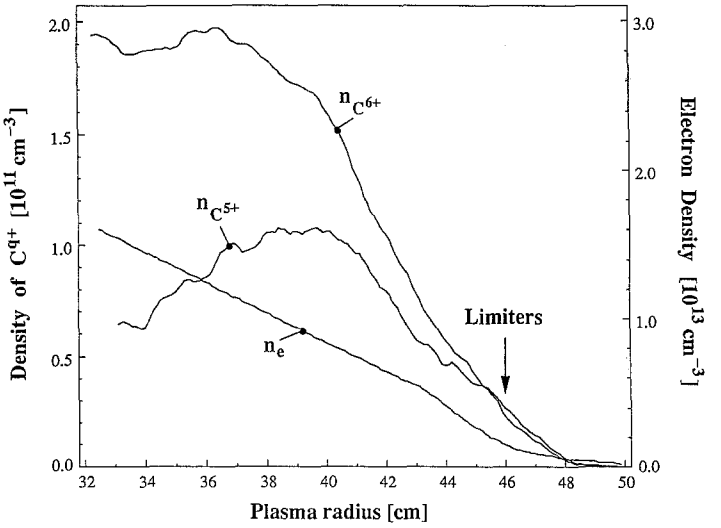

Fig. 8. Evaluated radial density profiles of C^{5+} and C^{6+}. The electron density profile being shown for comparison has been measured by means of HCN laser interferometry and Li beam diagnostics using a laser-blow-off-technique

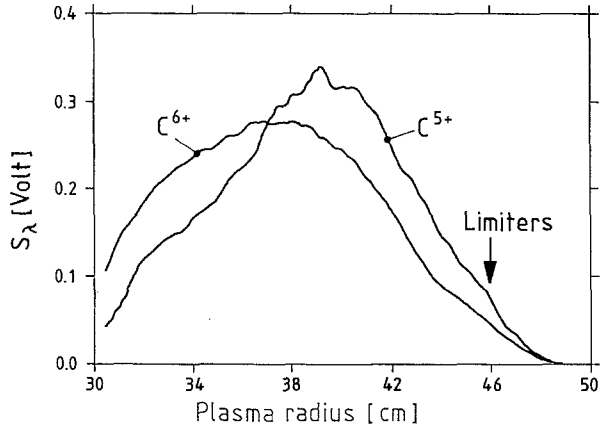

Fig. 7. Measured radial emission profiles of the Li beam activated CX-radiation of C^{5+} (TEXTOR shot #39510) and C^{6+} (#39505) before evaluation

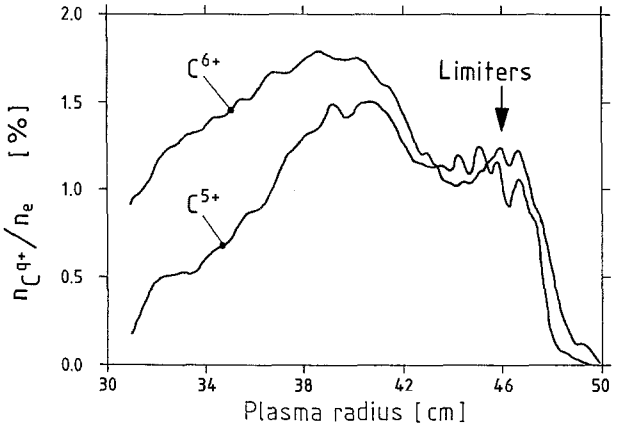

Fig. 9. Concentrations of C^{5+} and C^{6+} relative to the local electron density

the pulsed Li^0 beam of the $C^{5+} \rightarrow C^{4+}$ CX line at 494.5 nm is clearly visible. Here, the radial observation position was 40 cm outward of the plasma center, but the signal to background ratio changes only within a factor of two over the total scanning range. Modulation depths of up to 25% have been achieved with the lithium flux densities currently available.

Radial emission profiles have been measured by scanning the movable mirror with a frequency of 1 Hz over the interesting plasma radius interval of $R=$ 30–50 cm. Three complete scans can be made during the 1.5 s flat-top phase of an ohmically heated discharge. The modulated parts of these profiles, averaged over the flat-top interval, are shown in Fig. 7 for C^{5+} (#39510) and C^{6+} (#39505). Application of the lithium beam composition modelling (Sect. 2) together with absolute calibration of the CXS emission signals and the measured beam current results in the absolute density profiles of the respective ion species. Figure 8 shows such evaluated profiles, which are derived from the emission profiles of Fig. 7. Our evaluation procedure is believed to yield the relative radial dependence of impurity densities within $\pm 10\%$, while errors as large as a factor of two can occur for the absolute numbers, as has been estimated by varying the number of involved Li(*nl*) states and cross sections within their respective error limits. Figure 9 shows the corresponding impurity concentrations, i.e. their fractions of the local electron density.

5. Discussion and Outlook

In a carbonized machine, carbon and oxygen are the main impurities. The behaviour of the TEXTOR plasma has been studied in detail under such wall conditions e.g. in [23]. In a typical ohmically heated discharge, as employed for the Li-CXS experiments presented here, the overall carbon concentration is expected to be of the order of

1–3%, and the oxygen content roughly 0.2–0.6% of the electron density. Assuming the existence of only fully stripped C^{6+} ions in the plasma center and an approximately uniform distribution of C impurities across the minor plasma radius, the peak concentration of C^{6+} measured with Li-CXS might be compared with the total carbon content in the torus volume during the respective shot. The latter quantity is recorded on a standard basis at TEXTOR by analyzing the spectrum of the plasma's soft X-ray continuum radiation [23, 24]. In our case, the overall carbon concentration has been 1.9% (shot #39505), which shows a satisfactory agreement with a peak concentration of 1.8% C^{6+} as obtained from the here presented measurements. For the first time, absolute concentrations of several ionic states of carbon have been measured spatially resolved in the outermost 20 cm of a tokamak plasma by means of Li-CXS. The experimental knowledge of stationary radial impurity profiles together with the carbon source fluxes on limiter surfaces permits a more detailed study of the carbon transport behaviour than so far achievable. A first attempt to utilize Li-CXS results for explaining the transport of carbon into the plasma center is presented in [25].

Finally, we note that we also succeeded in measuring the temperatures of C^{5+} and C^{6+}. The CXS radiation intensity was sufficient to narrow the spectral resolution of the spectrometer such, that profiles of the resonance lines could be analyzed. Corresponding results will be published soon. Similar studies of plasmas with additional heating are scheduled for the near future, to further explore the potential of Li-CXS.

Acknowledgement. Participation of the TU Wien group has been supported by Kommission zur Koordination der Kernfusionsforschung at the Austrian Academy of Sciences.

References

1. H. Winter: Comments At. Mol. Phys. **12**, 165–195 (1982)
2. A. Pospieszczyk, F. Aumayr, H.L. Bay, E. Hintz, P. Leismann, Y.T. Lie, G.G. Ross, D. Rusbüldt, R.P. Schorn, B. Schweer, H. Winter: J. Nucl. Mater. **162–164**, 574–581 (1989)
3. H.L. Bay, E. Hintz, P. Leismann, D. Rusbüldt, F. Aumayr, H. Winter: Proc. 14th Europ. Conf. on Controlled Fusion Plasma Physics, Madrid (1987) p. 1276, and KFA Report Jül-2139, July 1987
4. P. Leismann: PhD thesis, Ruhr-Universität Bochum, December 1987
5. F. Aumayr, H. Winter: Ann. Phys. **42**, 228–238 (1985)
6. K. Kadota, K. Tsuchida, Y. Kawasumi, J. Fujita: Plasma Physics **20**, 1011–1023 (1978)
   K. McCormick and the ASDEX Team: Rev. Sci. Instrum. **56**, 1063–1065 (1985)
7. J. Fujita, K. McCormick: Proc. 6. Int. Conf. on Controlled Fusion and Plasma Physics, Moscow 1973, p. 191
   K. McCormick: In *Proceedings of "Basic and Advanced Diagnostic Techniques for Fusion Plasmas"*, Varenna 1986, pp. 635–656
8. U. Rebhan, N.J. Wiegart, H.-J. Kunze: Phys. Lett. **85A**, 228–230 (1981)
9. V.V. Afrosimov, Y.S. Gordeev, A.N. Zinov'ev: Sov. Phys. Techn. Phys. Lett. **3**, 39–40 (1977)
   R.C. Isler: Phys. Rev. Lett. **38**, 1359–1362 (1977)
   R.J. Fonck, D.S. Darrow, K.P. Jähnig: Phys. Rev. A **29**, 3288–3309 (1984)
   P.G. Carolan, B.P. Duval, A.R. Field, S.J. Fielding, N.C. Hawkes, N.J. Peacock: Phys. Rev. A **35**, 3454–3471 (1987)
10. A. Brazuk, H. Winter, D. Dijkkamp, A. Boellaard, F.J. DeHeer, A.G. Drentje: Phys. Lett. **101A**, 139–141 (1984)
11. R.J. Fonck et al.: Loc. cit [9]
    R.J. Fonck: Rev. Sci. Instrum. **56**, 885–890 (1985)
    R.C. Isler: Nucl. Instrum. Methods **B9**, 673–678 (1985)
12. C.D. Boley, R.K. Janev, D.E. Post: Phys. Rev. Lett. **52**, 534–537 (1984)
13. M. Schneider: Diplomarbeit, TU Wien (1990)
14. W.L. Wiese, M.W. Smith, B.M. Miles: *Atomic Transition Probabilities*, Vol. II, NSRDS-NBS 22, US. National Bureau of Standards, Washington D.C. (1969)
15. R.K. Janev, H. Winter: Phys. Rep. **117**, 265–387 (1985)
16. R. Keller, P. Spaedtke, E. Noehmayer: Proc. Intern. Ion Engineering Congress, Kyoto 1985, p. 25–30
17. H.L. Bay, E. Dullni, P. Leismann: KFA-Report Jül-2062, May 1986
18. A. Pospieszczyk, G.G. Ross: Rev. Sci. Instrum. **59**, 605–609 (1988)
19. E. Graffmann: Private communication
20. H. Soltwisch: In Course and Workshop on basic and advanced Fusion Plasma Diagnostic Techniques, Vol. 2, ed. by P.E. Stott (CRC, Brussels 1987)
21. D.M. Goebel, R.W. Conn, W.J. Corbett, K.H. Dippel, K.H. Finken, W.B. Gauster, A. Hardtke, J.A. Koski, W. Kohlhaas, R.T. McGrath, M.E. Malinowski, A. Miyahara, R. Moyer, A. Sagara, J.G. Watkins, G. Wolf, the TEXTOR Team, and the ICHR Team: J. Nucl. Mater. **162–164**, 115–127 (1989)
22. E. Unterreiter et al.: To be published
23. J. Schlueter, E. Graffmann, L. Könen, F. Waelbroeck, G. Waidmann, J. Winter and the TEXTOR Team: Europhysics Conference Abstracts, 12th European Conference on Controlled Fusion and Plasma Physics, Budapest (1985) Part II, pp. 627–630
24. S. von Goeler, W. Stodiek, H. Eubank, H. Fishman, S. Grebenshchikov, E. Hinnov: Nuclear Fusion **15**, 301–311 (1975)
25. H.A. Claassen, R.P. Schorn, H. Gerhauser, E. Hintz: Proceedings of the 9th International Conference on Plasma–Surface Interactions in Controlled Fusion Research, Bournemouth (1990) to be published in J. Nucl. Mater.